Available online at www.sciencedirect.com
SCIENCE DIRECT®
Talanta 64 (2004) 830–835
Talanta
www.elsevier.com/locate/talanta

Single-step calibration, prediction and real samples data acquisition for artificial neural network using a CCD camera

N. Maleki*, A. Safavi*, F. Sedaghatpour

Department of Chemistry, College of Sciences, Shiraz University, Shiraz 71454, Iran

Received 29 September 2003; received in revised form 23 February 2004 ; accepted 27 February 2004
Available online 28 July 2004

Abstract

An artificial neural network (ANN) model is developed for simultaneous determination of Al(III) and Fe(III) in alloys by using chrome azurol S (CAS) as the chromogenic reagent and CCD camera as the detection system. All calibration, prediction and real samples data were obtained by taking a single image. Experimental conditions were established to reduce interferences and increase sensitivity and selectivity in the analysis of Al(III) and Fe(III). In this way, an artificial neural network consisting of three layers of nodes was trained by applying a back-propagation learning rule. Sigmoid transfer functions were used in the hidden and output layers to facilitate nonlinear calibration. Both Al(III) and Fe(III) can be determined in the concentration range of 0.25–4 $\mu g\,ml^{-1}$ with satisfactory accuracy and precision. The proposed method was also applied satisfactorily to the determination of considered metal ions in two synthetic alloys.

Keywords: Artificial neural network; CCD camera; Aluminum; Iron(III)

1. Introduction

There has been a rapid improvement in the technology of digital photography, both in terms of hardware and software performance. The strong indications are that this rapid development will continue over the coming years, fuelled by the need for cheap, high performance image acquisition for consumer products and the web [1,2]. The combination of digital photography and colorimetric tests potentially offers a route to high throughput qualitative and quantitative analytical measurements.

The use of digital imaging as a detector for colorimetric reactions has great potential for many applications which involve the production of chemical color changes. The spatial resolution of the digital images, which can be produced by modern digital cameras facilitates the use of extremely small reagent areas, which can save on expensive or unavailable reagents [3]. Digital camera is based upon the use of charge-coupled devices (CCDs). Hence, a digital camera can act as an analytical detector, and generates a vast amount of information per image. In addition, analysis times may be lowered by taking single image, rather than having to scan the spectrophotometer and change a large number of samples.

The use of artificial neural networks (ANNs) in chemometrics has increased during the last decade [4,5]. ANNs are important class of pattern recognizer that may have many useful chemometric applications [6,7]. The feed-forward neural networks trained by back-propagation of the errors have one obvious advantage; there is no need to know the exact form of the analytical function on which the model should be built. Therefore, ANNs are suitable for experimental conditions optimization since the relationship between evaluating indices and the experimental input parameters is complex, nonlinear and often cannot be expressed with a certain mathematical formula. Basic theory and application of ANN with back-propagation algorithm to chemical problems can be found in the literature [8–12].

Chemometric methods such as ANN need many samples for calibration and prediction set, which is time consuming with usual techniques such as spectrophotometry because of the increase in measuring time due to the need for the measurement of each sample separately.

* Corresponding author. Tel.: +98 711 2284822; fax: +98 711 2286008.
E-mail addresses: nmaleki@chem.susc.ac.ir (N. Maleki), safavi@chem.susc.ac.ir (A. Safavi).

0039-9140/$ – see front matter © 2004 Elsevier B.V. All rights reserved.
doi:10.1016/j.talanta.2004.02.041

By using CCD camera as the detection system, all calibration, prediction and real samples data can be obtained by taking a single image and this decreases the analysis time.

Chrome azurol S (CAS) is a sensitive reagent for the determination of aluminum. Kashkovskaia and Mutafin used Chrome azurol S to determine aluminum in steels and aluminum bronzes [13]. They measured the absorbance of the aluminum–chrome azurol S lake at 530 nm, where Beer's law is not obeyed. Choosing a wavelength of 567 nm for absorbance measurements, the calibration curve of aluminum–chrome azurol S complex was found to obey Beer's law from 0 to 1.2 $\mu g\,ml^{-1}$ Al [14]. Sensitive spectrophotometric methods for the determination of Fe(III), based on complexes with a triphenylammonium reagent, chrome azurol S or eriochrome cyanine R (ECR) are described by Marczenko and Kalowska [15] and Shijo et al. [16]. In most of the reported methods for the determination of Al(III), iron interferes [14–17]. The same is true for the interfering effect of Al(III) on Fe(III) determination [15]. In the last decade, the use of multivariate techniques such as partial least square regression has received considerable attention particularly for simultaneous determination of different species such as aluminum and iron [18,19].

The main purpose of this work is to use CCD camera for signal recording and application of ANN in simultaneous determinations. The proposed method was used for simultaneous determination of Al(III) and Fe(III) with chrome azurol S.

2. Experimental

2.1. Apparatus

Measurements of pH were made with a Metrohm 691 pH-meter using a combined glass electrode. A Reflecta Flectalux XM 18 was used as a light source. A Canon EOS D30 camera was used for taking pictures.

2.2. Reagents

All chemicals used were of analytical-reagent grade. Triply distilled water was used throughout. A stock solution (8×10^{-3} M) of CAS, was prepared by dissolving 0.0484 g of CAS (Fluka) in water and diluting to 10 ml in a standard flask. A stock solution (500 $\mu g\,ml^{-1}$) of Al(III) was prepared by dissolving 0.6928 g of Al $(NO_3)_3{\cdot}9H_2O$ (Merck) in water and diluting to 100 ml. A stock solution (500 $\mu g\,ml^{-1}$) of Fe(III) was prepared by dissolving 0.4305 g of $NH_4Fe(SO_4)_2{\cdot}12H_2O$ (Merck) in water and diluting to 100 ml. Acetic-acetate buffer (pH 6) was prepared by using acetic acid (1 M) and sodium hydroxide (1 M) solution [20]. Stock solution (500 $\mu g\,ml^{-1}$) of each interfering ion was prepared by dissolving an appropriate amount of the suitable salt.

2.3. Procedure

To a solution containing appropriate amounts of Al(III) and Fe(III) in a 5 ml volumetric flask were added 0.2 ml of stock CAS solution, 2 ml of buffer solution, and the solution mixture was made up to the mark with water. For each sample, ca. 2 ml of the above solution was transferred to cells. There were 50 cells as calibration, prediction sets and real samples sets. All data were obtained by taking an image. A program written in Visual Basic as software was used to convert colors to red (R), green (G) and blue (B) values and ANN, which was trained with the back-propagation of errors learning algorithm, processed these values. A back-propagation neural network having three layers was created with a Visual Basic software package.

3. Results and discussion

3.1. Principles of the method

The spectrophotometric sensitive methods for determination of aluminum and iron are based on systems, including triphenylmethane reagents, such as CAS. Chrome azurol S reacts with Al(III) and Fe(III) ions to form water soluble colored complexes. The intensities of the color of CAS–Al and CAS–Fe complexes depend on the concentration of CAS. Since the color of the above complexes is distinct, CCD camera can be used as a sensitive method for the determination of Al(III) and Fe(III).

3.2. Digital camera and digital color

The analytical data that a digital camera returns are a standard trichromatic response, with 8-bit red, green and blue channels, respectively. Hence a value is returned to the user ranging from 0 to 255 for each channel. The spectral power distribution of light source and the spectral reflectance curve of the object being analyzed both play an important role in the value of color obtained through each channel [21]. The colors returned by each of the three channels are referred to as subtractive colors [21,22]. It should be noted that the eye sees the converse of the color component that is primarily absorbed, e.g. if an object appears red, it is because this color is being reflected or transmitted by the object and the blue part of the spectrum is being absorbed [23].

The use of digital images opens the possibility of increased usage of processing by computer software without the need for time consuming analysis by conventional spectrophotometric techniques.

The data were analyzed by a program written in Visual Basic and was then transported to Excel.

In order to obtain RGB values of many samples simultaneously two methods were implemented. In one method, small flat-bottomed wells were illuminated from the bottom and were photographed. This technique is very similar to

Fig. 1. Schematic photo of calibration, prediction and real sets used.

the one used by Rose [24]. The problem with this method is the meniscus of the water surface and its consequent lensing effect, which destroys the homogeneity of the image. In addition, reflected light on the surface also poses color homogeneity problems. Teflon and other plastics show the same problems. These problems can be seen from the photos taken by Rose [24].

In order to solve the problems, regular disposable rectangular cells were placed in front of a white transparent plate and the plate was back illuminated by photographic lights. The images were taken from the front of the cells.

In order to get as many data as possible from one image, fifty 1-cm plastic disposable cells were cut in half and were placed in a vertical rack in five stages as shown in Fig. 1.

In order to correct the background, a custom white balance was set with the plate illuminated with the photographic light. This procedure is absolutely essential in obtaining high quality data.

3.3. Optimization of experimental variables

3.3.1. Effect of pH

The sensitivity and selectivity are dependent on the pH of the medium. Thus, the pH of solutions of Al and Fe complex were varied and R, G and B values were obtained. At pH 6 the difference of the RGB values was highest and this pH was thus used as the optimum pH.

3.3.2. Effect of concentration of indicator

Since CAS is dark yellow at pH 6, its color interferes with that of the complexes. In order to minimize this effect, same amounts of Al and Fe were separately added to different concentrations of CAS. At 3.2×10^{-4} M CAS the difference in RGB values was a maximum.

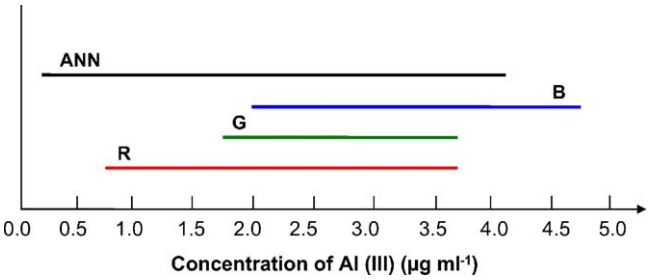

Fig. 2. Determination range of Al(III) using red, green, and blue bands obtained from aluminum standard solutions. Determination range using ANN obtained from aluminum standard solutions in the presence of iron.

3.4. Multivariate calibration with ANN

The data obtained from the image were processed by ANN, which was trained with the back-propagation of errors learning algorithm. The first step in the simultaneous determination of different metal ions by ANN methodology involves constructing the calibration set for the binary mixture Al(III)–Fe(III). In this study, the calibration and prediction sets were prepared randomly to reduce correlation between concentrations of Al(III) and Fe(III) (Tables 1 and 2). Twenty seven binary mixtures were selected as the calibration set and nine binary mixtures were selected as the prediction set for each ion. The training set of Al(III) and Fe(III) were between 0.25 and 4 $\mu g\,ml^{-1}$, respectively, in the calibration matrix. Also, the number of inputs was normalized between -3 and $+3$. Calibration set was used for construction of ANN model, and the independent test set was used to evaluate the quality of the model.

The overall predictive capacity of the model was compared in terms of relative standard error, R.S.E. which is defined as follows.

$$\text{R.S.E. (\%)} = 100 \times \left(\frac{\sum_{j=1}^{N} (\hat{C}_j - C_j)}{\sum_{j=1}^{N} (C_j)^2} \right)^{1/2}$$

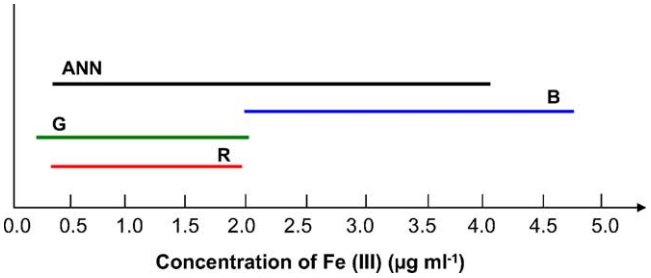

Fig. 3. Determination range of Fe(III) using red, green, and blue bands obtained from iron standard solutions. Determination range using ANN obtained from iron standard solutions in presence of aluminum.

Table 1
Composition of calibration set and RGB data

Input data			Concentration ($\mu g\,ml^{-1}$)	
R	G	B	Al(III)	Fe(III)
60	27	46	0.75	2.50
59	4	124	3.50	1.50
38	3	95	2.00	3.25
75	4	128	4.00	0.50
28	11	63	0.50	4.50
79	5	102	3.00	1.00
56	3	117	3.00	2.00
98	18	53	1.25	1.25
72	16	51	1.00	2.00
136	32	57	1.25	0.50
103	11	84	2.75	0.50
41	9	72	1.25	3.25
78	4	115	2.00	0.75
25	9	72	1.00	4.50
35	25	49	0.00	3.75
28	12	59	0.50	4.25
41	12	58	1.00	3.00
97	40	49	0.50	1.50
172	48	58	1.25	0.00
127	105	32	0.00	1.25
48	6	88	2.00	2.75
75	9	73	2.00	1.50
56	11	65	1.50	2.25
158	78	41	0.50	0.50
58	6	91	3.50	2.25
82	4	124	4.00	0.25
76	3	144	4.50	0.50

where C_j is j-th component of the desired target (real sample) and $\hat{C}_j$ is the j-th component of the output produced by the network (predicted sample).

To investigate the prediction ability of ANN, neural network models for individual component were also made with respect to output layer considered as a single node corresponding to the analyte [25]. The construction of these ANN models is summarized in Table 3. The structure of network was comprised of three layers, an input, a hidden and an output layer. The addition of an extra parameter, called bias, to the decision function increases its adaptability to decision problem it is designed to solve. In this structure, +1 was addition as a bias. There are several ways to optimize the parameters of a network [26–28]. One of them is constructed based on the minimum error of prediction of the testing set [29–32]. Training and testing of the network is a process of determination of the network's topology and optimization of its adjustable parameters where we seek the minimum of an error surface in multi-dimensional space. The optimum learning rate and momentum were evaluated by obtaining those, which yielded a minimum in error of prediction (of test set). The most versatile transfer function that can be used to model a variety of relationship is the sigmoidal type. In the present nonlinear system, sigmoid functions were found to be optimum for hidden and output layers. The number of nodes in the hidden layer was determined by training ANN with different number of nodes and then comparing the prediction errors from the test set.

Table 2
Composition of prediction set and RGB data

Input data			Concentration ($\mu g\,ml^{-1}$)	
R	G	B	Al(III)	Fe(III)
58	5	75	2.00	2.00
36	4	79	1.50	3.50
44	5	96	2.00	3.00
53	11	59	1.00	2.75
104	19	60	1.50	1.00
54	6	80	0.50	2.50
79	14	56	1.25	1.75
74	2	128	4.00	0.50
91	4	145	4.50	0.13

Table 3
Optimized parameters used for construction of ANN models

Parameter	Compound	
	Al(III)	Fe(III)
Input nodes	3	3
Hidden nodes	4	3
Output nodes	1	1
Learning rate	0.5	0.5
Momentum	0.08	0.2
Hidden layer function	Sigmoid	Sigmoid
Output layer function	Sigmoid	Sigmoid
Number of iterations	8675	1050

The training was stopped manually when the root mean square error of the test set remained constant after successive iteration. The optimum number of iteration cycles or epochs (one pass of all objects, 27 mixtures, through the network) for each component was also obtained. Fig. 4 shows a sample plot of RSEC and RSEP as a function of the number of iteration for Fe(III) components. Because there are several local minima, the algorithm was run from different starting values of initial weights to find the best optimum.

RSEP for Al and Fe were 4.8% and 5.6%. The reasonable relative standard error of prediction for each analyte indicates the accuracy of the proposed method (Table 4).

Table 4
Composition of prediction set and relative standard errors for analytes

Actual		Found	
Al(III)	Fe(III)	Al(III)	Fe(III)
2.00	2.00	1.87	2.25
1.50	3.50	1.44	3.55
2.00	3.00	1.90	2.96
1.00	2.75	0.99	2.51
1.50	1.00	1.33	0.98
0.50	2.50	0.39	2.40
1.25	1.75	1.32	1.72
4.00	0.50	4.08	0.54
4.50	0.13	4.30	0.19
R.S.E. (%)		4.80	5.61

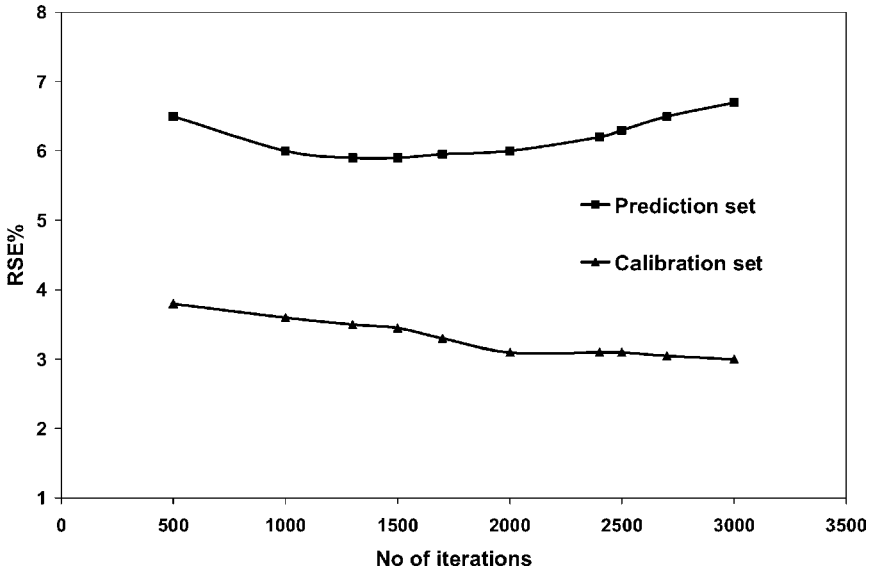

Fig. 4. Plots of RSEP (%) and RSEC (%) as a function of the number of iterations for Fe(III).

The concentration of both Al(III) and Fe(III) samples were between 0.25 and 4.50 μg ml^{-1}. We could use only R, G or B value for analysis but using each color band, limits the determination range. In order to broaden the determination range and also to simultaneously determine Al(III) and Fe(III), red, green, and blue bands in conjunction with ANN as a nonlinear method was used (Figs. 2 and 3).

3.5. Interferences

The selectivity was assessed by studying the influence of foreign ions on the determination of Al(III) and Fe(III). The effect of interfering ions at different concentrations was studied on RGB values of a solution containing 1.25 μg ml^{-1} of each analyte. The results are summarized in Table 5. The tolerance limit was defined as the concentration above which a change of more than three times of standard deviation was observed in the signals obtained for the analytes.

Table 5
Effect of various ions on the determination of 1.25 μg ml^{-1} Al(III) and 1.25 μg ml^{-1} Fe(III)

Ion added	Tolerance level (μg ml^{-1})
Mn(II), Co(II), Ni(II)	200
Cd(II)	5
Pb(II)	50
Ce(II)	100
Cu(II)	4
Cr(III), Cr(VI)	8
Cl^-, CH_3COO^-, Na^+, Br^-	500[a]
F^-, PO_4^{3-}, Citrate, Tartarate, Fe(II), Ga(III)	1.25

[a] Maximum concentration studied.

Table 6
Estimated and actual concentration of Al(III) and Fe(III) in synthetic alloys

Sample	Al(III) (μg ml^{-1})		Fe(III) (μg ml^{-1})	
	Actual	Found	Actual	Found
Ferro-aluminum	1.00	1.15 ± 0.04	3.00	2.77 ± 0.04
Recovery (%)		115		92.3
Ignition pin alloy[a]	0.75	0.75 ± 0.10	2.00	1.93 ± 0.01
Recovery (%)		100		96.5

[a] Containing 70.00 μg ml^{-1} Co(II), 16.00 μg ml^{-1} Zn(II), 2.00 μg ml^{-1} Fe(III), 0.75 μg ml^{-1} Al(III), 1.50 μg ml^{-1} Mn(II).

3.6. Real sample analysis

The proposed method was also applied to the determination of Al(III) and Fe(III) in synthetic alloys [33]. Eight cells were related to two real samples and their replication. The results are shown in Table 6. The good agreement between these results and known values indicates the successful applicability of the proposed method for simultaneous determination of Al(III) and Fe(III) in real sample.

Acknowledgements

The authors gratefully acknowledge the support of this work by Shiraz University Research Council.

References

[1] P.M. Epperson, J.V. Sweedler, R.B. Bilhom, G.R. Sims, M.B. Denton, Anal. Chem. 60 (1988) 282A.

[2] Oeean Optics (online), available from: http://www.oeeanoptics.com/homepage.asp (accessed 31 January 2000).
[3] P.M. Epperson, J.V. Sweedler, R.B. Bilhorn, G.R. Sims, M.B. Denton, Anal. Chem. 60 (1988) 327A.
[4] J. Zupan, J. Gasteiger, Anal. Chim. Acta 248 (1991) 1–3.
[5] G. Kateman, Cemom. Intell. Lab. Syst. 19 (1993) 135–142.
[6] J.R. Long, V.G. Gregoriou, P.J. Gemperline, Anal. Chem. 62 (1990) 1791.
[7] J. Schuur, I. Gasteiger, Anal. Chem. 69 (1997) 2398.
[8] B.J. Wythoff, Chemom. Intell. Lab. Syst. 18 (1993) 115.
[9] P.A. Jansson, Anal. Chem. 63 (1991) 357A.
[10] J. Zupan, J. Gasteiger, Angew. Chem. Int. Ed. Engl. 32 (1993) 503.
[11] W. Guo, P. Zhu, H. Brodowsky, Talanta 44 (1997) 1995–2001.
[12] Y. Ni, C. Lui, Anal. Chim. Acta 396 (1999) 221–230.
[13] E.A. Kashkovaskaia, I.S. Mustafin, Zavodsk. Lab. 24 (1985) 1319.
[14] P. Pakains, Anal. Chim. Acta 32 (1965) 57–63.
[15] Z. Marczenko, H. Kalowska, Anal. Chim. Acta 123 (1981) 279–287.
[16] Y. Shijo, T. Takeuchi, Bunseki Kagaku 20 (1971) 980.
[17] R.M. Dagnall, T.S. West, P. Young, Analyst 90 (1965) 13.
[18] A.R. Coscione, J. Carlos de Andrade, R.J. Poppi, C. Mello, B.V. Raij, M.F. de Abreu, Anal. Chim. Acta 423 (2000) 31–40.
[19] A.R. Coscione, J. Carlos de Andrade, R.J. Poppi, Analyst 127 (2002) 135.
[20] J. Lurie, Handbook of Analytical Chemistry (English translation), Mir, Moscow, 1975.
[21] E.J. Ciorgianni, T.E. Madden, Digital Color Management: Encoding Solution, Addison Wesley, USA, 1998, p. 9.
[22] http://developer.apple.com/documentation/GraghicsImaging/Conceptual/ManagingColorSync/ColorSync.pdf.
[23] L. Byrne, J. Barker, G. PennarunThomas, D. Diamond, Trends Anal. Chem. 19 (2000) 517.
[24] A.V. Lemmo, J.T. Fisher, H.M. Geysen, D.J. Rose, Anal. Chem. 69 (1997) 543.
[25] F. Despagne, D.L. Massart, Analyst 123 (1998) 157R.
[26] J.R.M. Smits, W.J. Melssen, L.M. Buuydens, G. Kateman, Chemom. Intell. Lab. Syst. 22 (1992) 165.
[27] J.H. Wikel, E.R. Dow, Bioorg, Med. Chem. Lett. 3 (1993) 645.
[28] M. Bos, A. Bos, W.E. Van der linden, Analyst 118 (1993) 323.
[29] M. Shamsipur, B. Hemmateenezhad, M. Akhond, Anal. Chim. Acta 461 (2002) 147.
[30] G. Absalan, A. Safavi, S. Maesum, Talanta 55 (2001) 1227.
[31] M. Baret, D.L. Massart, P. Fabry, F. Conesa, C. Eichner, C. Menardo, Talanta 51 (2000) 863.
[32] Y.B. Zeng, H.P. Xu, H.T. Liu, K.T. Wang, X.G. Chen, Z.D. Hu, B. Fan, Talanta 54 (2001) 603.
[33] http://chemistry.csudh.edu/oliver/chemdata/alloys.htm.